Jurnal
Teknologi

Full Paper

ELECTROLESS QUATERNARY NI-CU-CO-P ALLOY DEPOSITION MECHANISM IN ACIDIC BATH USING CYCLIC VOLTAMMETRY MEASUREMENT

Article history
Received
30 August 2016
Received in revised form
13 November 2016
Accepted
13 March 2017

Mohd Nor Azran[a], Muhamad Khaizaki[a], Muhammad Alif[a], Muhammad Zaimi[a*], Mohd Asyadi 'Azam[a], Mohd Shahir Kasim[a], Mohd Sanusi Abdul Aizi[a], T Joseph Sahaya Anand[a], Che Hassan Che Haron[b], Jaharah A. Ghani[b]

[a]Faculty of Manufacturing Engineering, Universiti Teknikal Malaysia Melaka, 76100 Melaka, Malaysia
[b]Department of Mechanical and Material Engineering, Faculty of Engineering, Universiti Kebangsaan Malaysia, 43600 Selangor, Malaysia

*Corresponding author
mdzaimi@utem.edu.my

Graphical abstract

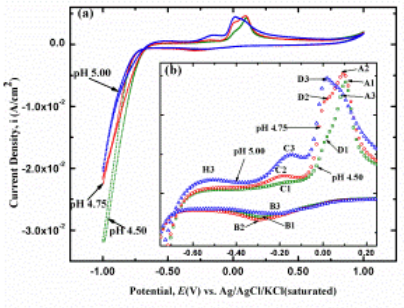

Abstract

Quaternary nickel alloy of Ni-Co-Cu-P has been successfully deposit on Fe substrate for corrosion resistant material. However, the reaction mechanism of quaternary nickel alloy deposition is less known and requires investigation. In this study, using similar bath component is used to produce electroless Ni-Cu-Co-P alloy. Cyclic voltammetry (CV) study is done in various plating bath component at bath pH 4.50, 4.75 and 5.00. A coating of Ni-Cu-Co-P alloy was deposited on a Fe substrate to evaluate surface morphology and composition. From CV results, higher bath pH, increases the [$H_2PO_2^-$] oxidation peak and shifted the oxidation potential towards less noble potential. The reduction potential of the Ni alloy moved to noble potential, hence, elevate deposition rate from 3.95 to 5.95 µm/hr. The Ni-Cu-Co-P alloy composition on Fe substrate in descending manner is Ni (68.55 – 82.09 wt%), Cu (14.11 – 27.80 wt%) and Co (1.32 - 1.52wt%). The P content remained lower than 3.00 wt%. Hence, Co act as reaction inhibitor, while Cu act as both reaction accelerator and stabilizer.

Keywords: Electroless quaternary nickel alloy deposition, deposition mechanism, cyclic voltammetry, surface morphology, corrosion resistant coating

1.0 INTRODUCTION

Nickel alloy deposition by reaction between reducing agent and nickel ion without current density applied on a substrate is called electroless deposition. The reaction produced highly activated nickel coating surface that promotes continuous deposition reaction, hence also referred as autocatalytic deposition. The reducing agent has secondary reaction on the catalytic surface of nickel, providing extra element to the nickel coating surface producing a binary alloy. For example, the use of hypophosphite ion, [$H_2PO_2^-$] as reducing agent will co-deposit phosphorous, P onto nickel surface, becoming a Ni-P alloy. The existence of P benefiting the nickel coating by improving the several properties such as hardness, wear resistance, corrosion resistance in seawater and many more. Furthermore, the electroless deposition reaction can be done uniformly on any type and shape of substrates, as long as the surface is activated. This gives advantages to this method to be applied on various fields, including electronics, automobile, and chemical [1].

The addition of another metal element in Ni-P alloy can change the properties of the alloy [2]. This can easily be done by adding metal salts such as Cu salts into the electroless Ni-P plating bath solution. Thus, it is possible to produce ternary and quaternary nickel alloy using electroless deposition method. The Cu addition in Ni-P alloy increases electrical conductivity and corrosion resistance will reducing the magnetic coercivity [3]. Co addition has similar effect as Cu on Ni-P alloy except the increase of magnetic coercivity [4].

Quaternary alloy from electroless nickel plating bath is produce adding another two metal salts in the plating bath. One of the most famous quaternary alloy is Co-Ni-Mn-P which is used as a vertical memory device of a hard drive [1, 5]. In previous study, an electroless quaternary nickel alloy of Ni-Cu-Zn-P is produced by adding Cu and Zn salts into the electroless Ni-P plating bath [6]. There are also reported that the incorporation of electroless Ni-W-Cu-P alloy on carbon fibers for electromagnetic shielding application [17].

Most of the electroless nickel alloy deposition mechanism describes the effect of various parameter including reducing agent, complexing agent, buffering agent, stabilizer, accelerator and inhibitor concentrations on the deposit properties [18, 19]. Several mechanisms of electroless nickel alloy deposition is done using electrochemical method such as electrochemical impedance spectroscopy (EIS), polarization curve measurement, open circuit potential, and cyclic voltammetry. The polarization curve measurement during electroless nickel deposition has been done by L.M. Abrantes *et al*. in 1994 [7]. Nevertheless, it requires to be done in both anodic and cathodic polarization. The samples used are also have reaction occurred during measure, hence may not acquire accurate data. The EIS study of the electroless nickel deposition is done by Guofeng *et al.* [8]. The EIS measurement result display charge transfer resistance between surface of a substrate and electroless Ni-P plating bath solution. Still, the in terms of electroless quaternary plating bath solutions, it is difficult to observe the reaction of other metal ion with [$H_2PO_2^-$] on a substrate surface. The cyclic voltammetry on the other hand, can observed a similar result as polarization curve measurement, showing both oxidation and reduction reaction with much stable result. This study is done earlier by Aina Hung and Ker-Ming Chen [9], using [$H_2PO_2^-$] to reduce [Cu^{2+}]. Other researcher also has done similar study with electroless Ni-Zn-P deposition [10]. However, the electroless quaternary nickel alloy deposition study by cyclic voltammetry is required to be studied as different metallic ion has different effect on the deposition.

In this study, the mechanism of electroless quaternary Ni-Cu-Co-P deposition in acidic plating bath pH is studied using cyclic voltammetry measurement. The electroless Ni-Cu-Co-P alloy deposition is validated by producing the coating using similar plating bath solution at various pH.

2.0 METHODOLOGY

Cyclic voltammetry (CV) measurement is done in classical three electrode cell with Ag/AgCl/KCl (saturated) as reference electrode. Two graphite electrodes are used as working electrode and counter electrode. The plating bath solutions is used as test solution as per Table 1.

Each bath pH is set to 4.50, 4.75 and 5.00. Measurement is done at 298K, scanning rate 1 mV/s from -1.00V to 1.00V for three cycles. Only one cycle loop is taken for each measurement for this discussion from comparison of second and third cycle loop. The plating bath composition is decided based on previous studies [11].

Electroless quaternary nickel alloy is done on iron substrate (Fe, 99.5%) in the plating bath solution similar as Bath #1 in Table 1. The iron substrate is first cleaned and degreased using distilled water and ethylic alcohol in sequence. Then, the substrate is rinsed using distilled water again before immersing into diluted HCl aqueous solution for 120 s for etching. The substrate is then rinsed heavily using distilled water and then immersed into electroless plating bath solution. The deposition is done for 3600 s at 358K. The deposition is done each with different plating bath pH of 4.50, 4.75 and 5.00. The plating bath pH is adjusted using ethanoic acid.

Table 1 Bath composition of electroless nickel alloy deposition

	Bath #					
Composition	**1**	**2**	**3**	**4**	**5**	**6**
$NiSO_4.6H_2O$ (M)	0.10	-	-	0.10	0.10	0.10
$CoSO_4.7H_2O$ (M)	-	0.01	-	0.01		0.01
$CuSO_4.5H_2O$ (M)	-	-	0.001		0.001	0.001
$NaH_2PO_2.H_2O$ (M)	0.28	0.28	0.28	0.28	0.28	0.28
$Na_3C_6H_5O_7.2H_2O$ (M)	0.20	0.20	0.20	0.20	0.20	0.20
NH_4SO_4 (M)	0.50	0.50	0.50	0.50	0.50	0.50

Composition of the electroless Ni-Cu-Co-P alloy is determined using X-ray Fluorescence (XRF) measurement. Deposition rate of electroless deposition is determined by weight difference calculation method. Surface morphology is observed using Scanning Electron Microscope (SEM).

3.0 RESULTS AND DISCUSSION

In Bath #1 Ni-P solutions (Figure 1), A1, A2 and A3 anodic current peaks represent the Ni-P alloy dissolution. B1, B2 and B3 represent reduction current valley of the Ni-P alloy on graphite. The A1 (43.2mV) and A3 (35.8mV) anodic current peaks have near value of 3.67 × 10^{-4} Acm^{-2} and 3.81 × 10^{-4} Acm^{-2} respectively. However, at pH 5.00, the anodic current peak A3 (45.6mV) reduces significantly to 1.17 × 10^{-4} Acm^{-2}. The C1 and C2 cathodic current valleys are -

3.59 x 10^{-4} Acm^{-2} and -3.70 x 10^{-4} Acm^{-2}, are significantly lower than C3, at 1.17 × 10^{-4} Acm^{-2}. The reduction potential shifted towards noble potential as bath pH increases, where B1, B2 and B3 is approximately -470mV, -430mV and -370mV respectively. Although the $[H_2PO_2^-]$ oxidation peak, H cannot be accurately determined, it can be seen during initial anodic sweep that the peak H is shifted towards less noble potential with the elevation of bath pH. Hence, at higher bath pH, the bigger difference between Ni-P reduction potential and $[H_2PO_2^-]$ oxidation potential promotes faster deposition.

The anodic peaks of A and C for Co-P bath (Bath #2) are the oxidation of Co-P alloy in Figure 2. The anodic peak C is the formation of Co-P oxidation layer and the anodic peak A is the dissolution of the oxide layer. The dissolution potential of Co-P alloy is 388mV, 383mV and 455mV in order of peak A1, A2 and A3. The existence of C1 (60.3mV), C2 (57.9mV) and C3 (60mV) shows that a stable Co-P oxide layer may have been produced during anodic sweep. The cathodic sweep of the CV exhibits two different reduction valleys. The cathodic valley D is the reduction of Co-P alloy, where D3 is the noblest potential at approximately -418mV, followed by D2 and D1at -428mV and -435mV respectively. On the other hand, cathodic valley B is -202mV (B1), -148mV (B2) and -218mV (B3). Also, slight shift of peak H to less noble potential can be observed at elevated bath pH. Thus, it can be deduced that higher plating bath pH promotes Co-P deposition based on cathodic valley D. The cathodic valley B occurrence may be caused by oxidation of Co-P alloy on the counter electrode instead of working electrode.

The Bath #3 in Figure 3 displays the decrease of reduction potential of Cu-P from B1 (-284 mV), B2 (306mV) to B3 (343mV). The $[H_2PO_2^-]$ oxidation displays similar potential reduction as other bath with the rise of bath pH. The trend shows that Cu-P is less deposit in higher bath pH which related with the stability of $[Cu^{2+}]$ complex at elevated bath pH despite peak H potential declination. The oxidation peak A1 (99.3mV), A2 (89.6mV) and A3 (53.6mV) in Figure 3 reflect to oxidation potential of Cu-P. The Cu-P is a barrier resistant alloy, exhibits no secondary oxidation peak compare to Co-P. The anodic peak A1 has the highest current density and the most noble dissolution potential compare to A2 and A3 peak. The noble dissolution potential and current density is may affected by the amount of Cu-P deposited on the graphite surface at lower bath pH.

Figure 4 present the Bath #4, electroless Ni-Co-P bath CV measurements. At pH 4.50 and pH 4.75, the reduction occurs at -319mV and -350mV, sequentially. On the other hand, the reduction potential in pH 5.00 bath shifted towards nobler potential of -299mV. Compare to Co-P bath #2, there is no secondary reduction appeared during the CV measurement. The $[H_2PO_2^-]$ oxidation peak H shows less change of potential. The A1 (28.3mV), A2 (13.6mV) and A3 (6.29mV) anodic peaks also interpret as the dissolution potential of the Ni-Co-P alloy. The plating bath pH 5.00 displays secondary oxidation peak C3 (-252mV), similar as in Co-P bath. Thus, shows that at higher bath pH, Co content increases, while P content decreases [12]. Furthermore, the existence Co in the Ni-P alloy matrix may improve the dissolution resistance by providing stable oxide layer [13].

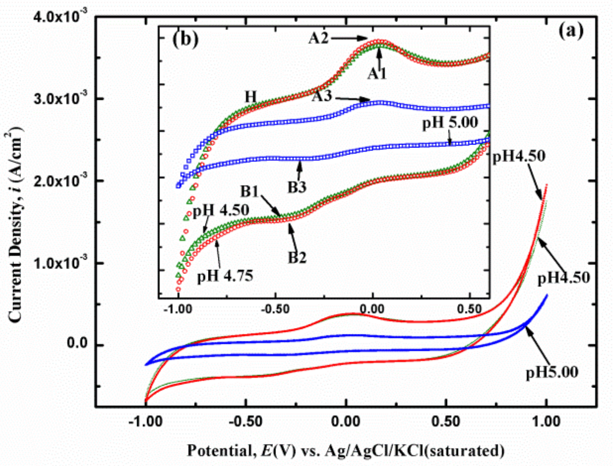

Figure 1 Cyclic voltammetry measurements of acidic electroless Ni-P bath (Bath #1); (a) Full range, (b) Magnified

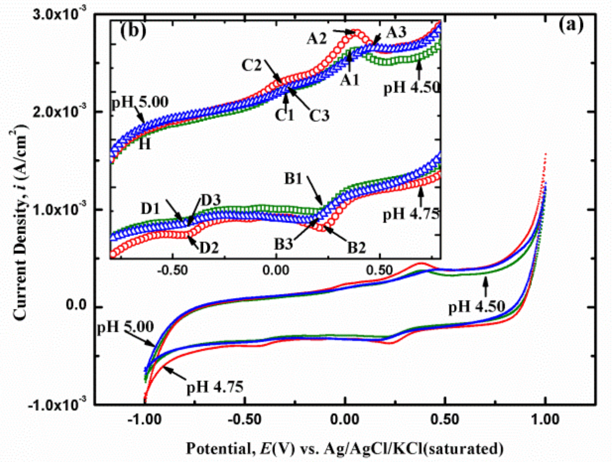

Figure 2 Cyclic voltammetry measurements of acidic electroless Co-P bath (Bath #2); (a) Full range, (b) Magnified

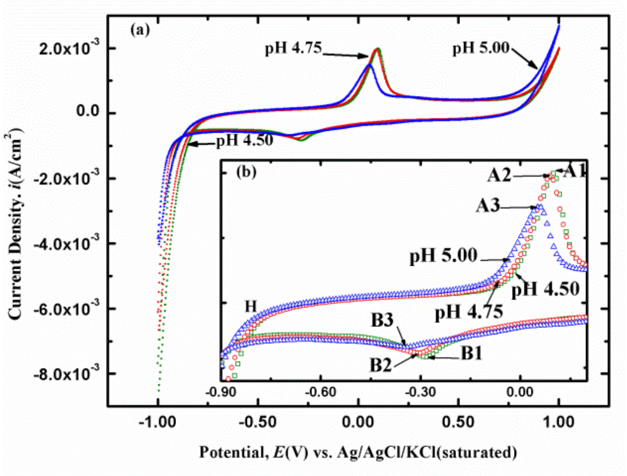

Figure 3 Cyclic voltammetry measurements of acidic electroless Cu-P bath (Bath#3); (a) Full range, (b) Magnified

In Bath #6, the CV measurement results of electroless Ni-Cu-Co-P deposition displays three anodic peak and one reduction valley for each bath pH (Figure 5). The $[H_2PO_2^-]$ oxidation peak is clearly seen at -508mV during CV measurements in pH 5.00 compare to other bath pH. The reduction potential of electroless Ni-Cu-Co-P alloy in pH 5.00 bath is -213mV (B1), more noble than of bath pH 4.50 (B1, -279mV) and bath pH 4.75 (B2, 294mV). Thusly, higher deposition rate of Ni-Cu-Co-P is expected at pH 5.00 bath compare to pH 4.50 and pH 4.75. In pH 4.50 bath, the influence of Co in the Ni alloy is lower than in higher pH due to low peak C1 at-169mV. The effect Co increases at C2 (-176mV) and C3 (-146mV). Hence, Co content the Ni alloy is suspected to heighten at high bath pH. Also, the oxidation peak C3 may shows stable oxide layer before undergo dissolution at D3 (16.2mV) and then, A3 (84.6mV). The D peak can be influenced by Ni alloy species dissolution from comparison with other bath. The dissolution potential of various baths increasing in sequence from Ni-Co-P, Ni-P, Co-P, Ni-Cu-P and Cu-P bath.

The deposition rate (μm/hr.) for electroless Ni-Cu-Co-P deposition in bath pH 4.50, 4.75, and 5.00 is approximately 3.55, 4.50 and 5.95 μm/hr. respectively. As a result, the increase of bath pH accelerates the deposition rate by improving the $[H_2PO_2^-]$ oxidation such shown in Figure 6.

The elemental composition of electroless Ni-Co-Cu-P deposit from various bath pH determined by XRF is shown in Table 2. The Co content in Ni alloy is the lowest among other element and slightly increase with higher bath pH. This conclude that $[Co^{2+}]$ existence in acidic bath act as inhibitor for deposition reaction where at 0.01M concentration only produces minimal Co content in the Ni alloy.

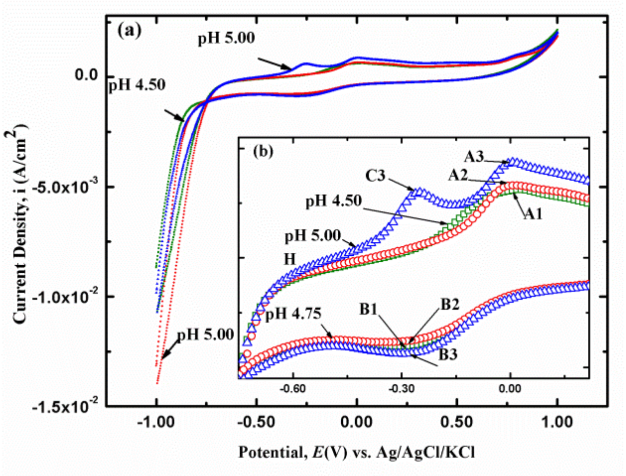

Figure 4 Cyclic voltammetry measurements of acidic electroless Ni-Co-P bath (Bath #4); (a) Full range, (b) Magnified

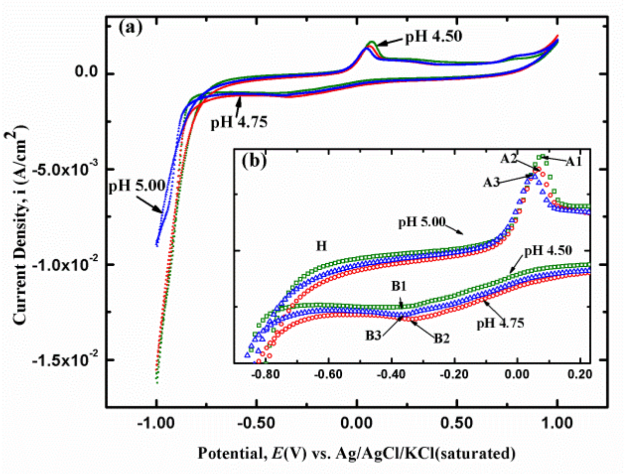

Figure 5 Cyclic voltammetry measurements of acidic electroless Ni-Cu-P bath (Bath#6); (a) Full range, (b) Magnified

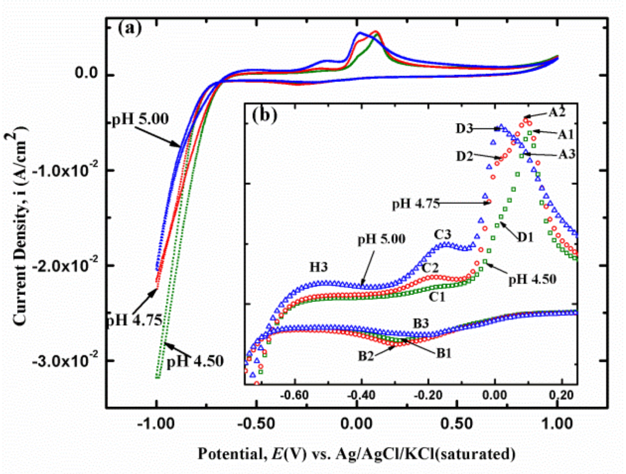

Figure 6 Cyclic voltammetry measurements of acidic electroless Ni-Cu-Co-P bath (Bath #1); (a) Full range, (b) Magnified

In case of Cu, despite added in low concentration (0.001M), the Cu content is significantly higher than Co content at maximum 27.80wt%. This proves that, Cu deposits better in low concentration and low bath pH due to its behavior acts as accelerator and stabilizer with the presence of Ni [14]. The P content remained lower than 3 wt%, which shows that the P co-deposition is lesser with the existence of $[Cu^{2+}]$. The reduction of Cu content at pH 4.75 compare to pH 5.00 is due to interaction between [Ni2+], [Cu2+] and [Co2+], competing for deposition on the surface. This can be related to changes of deposition potential in Figure 6 CV results where B2 is more towards Ni deposition instead of Cu and Co.

In Figure 7, the surface of electroless Ni-Cu-Co-P deposit has a compact and uniform surface due to absence of pores [1]. The addition of Cu which accelerates and stabilizes the deposition reaction produces fine and dense Ni alloy deposit.

The $[H_2PO_2^-]$ oxidation during electroless deposition reaction as suggested by Van den Meerakker requires adsorption, dehydrogenation and oxidation with hydroxyl group attack represent by equation (1),(2) and (3) respectively [15]. The Ni, Cu and Co deposition equation is (4), (5) and (6) in sequent. Equation (7) is the P co-deposition [1].

$$\mathrm{H_2PO_2^-} \rightarrow \mathrm{H_2PO_2^-}_{\mathrm{ad}} \quad (1)$$

$$\mathrm{H_2PO_2^-}_{\mathrm{ad}} \rightarrow \mathrm{HPO_2^-}_{\mathrm{ad}} + \mathrm{H_{ad}} \quad (2)$$

$$\mathrm{HPO_2^-}_{\mathrm{ad}} + \mathrm{OH_{ad}^-} \rightarrow \mathrm{H_2PO_3^-}_{\mathrm{ad}} + \mathrm{e^-} \quad (3)$$

$$\mathrm{Ni^{2+}} + 2\mathrm{e^-} \rightarrow \mathrm{Ni} \quad (4)$$

$$\mathrm{Cu^{2+}} + 2\mathrm{e^-} \rightarrow \mathrm{Cu} \quad (5)$$

$$\mathrm{Co^{2+}} + 2\mathrm{e^-} \rightarrow \mathrm{Co} \quad (6)$$

$$\mathrm{H_2PO_2^-} + 2\mathrm{H^+} + \mathrm{e^-} \rightarrow 2\mathrm{H_2O} \quad + \quad \mathrm{P} \quad (7)$$

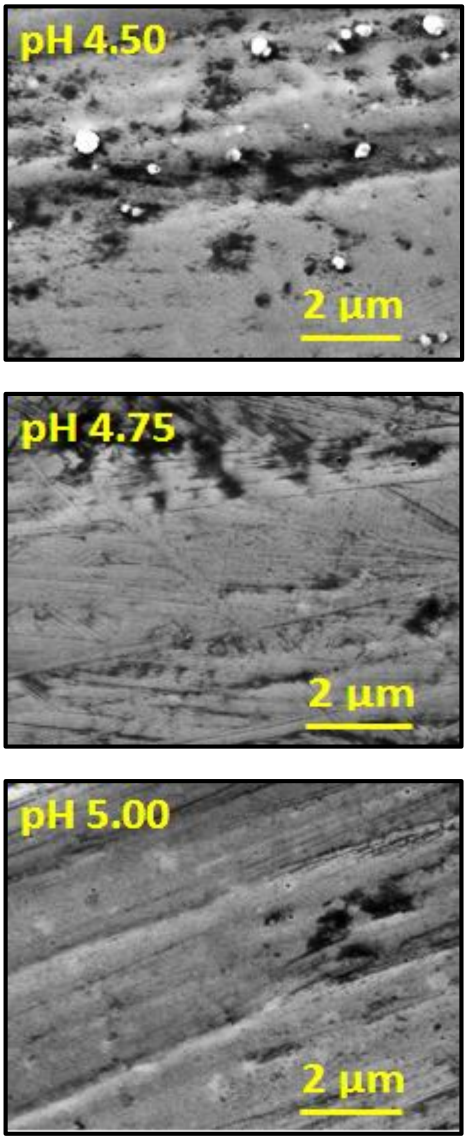

Figure 7 SEM micrograph of electroless Ni-Cu-Co-P alloy deposit

The CV results can observe the $[H_2PO_2^-]$ oxidation, where at higher bath pH, the hydroxyl concentration increases, thus, accelerate the oxidation reaction. In the first layer of deposition, it is understandable that Ni is the first deposited before other elements. Once the first layer of Ni is deposited, the surface is highly active for $[H_2PO_2^-]$ to attach and oxidized (Figure 8(a)). During the initial deposition, Co also supposed to be deposited, however, the aggressive Ni deposition reaction overtake the first layer. The second layer of the deposition can be either from $[Ni^{2+}]$ or $[Cu^{2+}]$ or $[Co^{2+}]$ reduction (Figure 8(b)). The Ni deposition followed by Cu deposition is the dominant reactions in this system [16]. The $[Co^{2+}]$ reduction is the slowest given the surface has high Cu content that lower the $[H_2PO_2^-]$ oxidation reaction. This also affects the co-deposition of P, since it requires highly catalytic surface of Ni and Co (Figure 8(c)) [1].

Table 2 Composition of electroless Ni-Cu-Co-P alloy in from various bath pH

	pH 4.50	pH 4.75	pH 5.00
Ni(wt%)	68.55	82.09	74.42
Co(wt%)	1.32	1.39	1.52
Cu(wt%)	27.80	14.11	22.11
P(wt%)	2.33	2.42	1.96

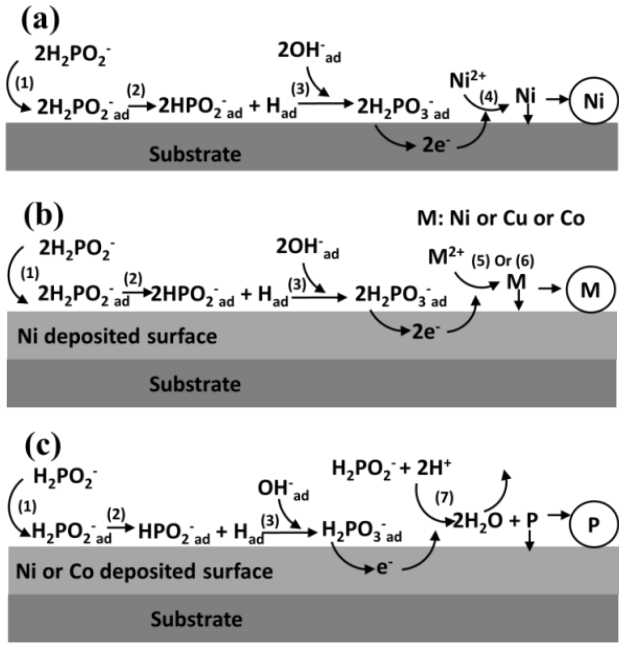

Figure 8 Deposition mechanism of electroless Ni-Cu-Co-P alloy deposition in acidic bath. (a) Ni deposition (b) Ni or Cu or Co deposition (c) P co-deposition

4.0 CONCLUSION

The deposition rate elevated at high bath pH due to higher concentration of hydroxyl which increases the $[H_2PO_2^-]$ oxidation reaction. Hence, $[H_2PO_2^-]$ oxidation peak can be observed increasing and its potential shifted toward less noble potential. Also, the reduction potential of Ni-Cu-Co-P alloy becomes nobler with higher bath pH contribute the faster deposition rate.

The acidic bath increases the deposition of Cu in the Ni alloy matrix with $[Cu^{2+}]$ that acts as deposition accelerator and stabilizer when added in small concentration. Although the $[Co^{2+}]$ can be reduced by $[H_2PO_2^-]$, it acts as inhibitor in electroless Ni-Cu-Co-P bath. The P content from all three baths is lower than 3.00 wt%. The high Cu content in the Ni-Cu-Co-P alloy decreases the Co reduction and P co-deposition. The Co content is significantly lower than Cu content in Ni-Cu-Co-P alloy. All three cations, [Ni2+], [Cu2+] and [Co2+], are competing for deposition on the surface and can be observed using CV measurements. Hence, CV measurement can be used to understand reaction mechanism of electroless quaternary nickel alloy deposition.

Acknowledgement

The authors are utmost grateful for the research grant RAGS/2013/FKP/TK04/01/B00028 funded by Ministry of Higher Education. Special gratitude to Faculty of Manufacturing Engineering, Universiti Teknikal Malaysia Melaka for providing facilities and technical support personnel.

References

[1] G. O. Mallory, J. B. Hajdu. 1990. *Electroless Plating: Fundamentals and Applications.* AESF, Orlando, Florida.

[2] Zaimi, M., Azam, M. A., Sofian, Azizul Helmi and Noda, K. 2015. Electrochemical Impedance Behavior of Various Composition Quaternary Ni Alloy in 3.5wt% NaCl. *Applied Mechanics and Materials*. 761: 401-411.

[3] Georgieva, J. and Armyanov, S. 2003. Factors Affecting the Electroless Deposition of Ni-Cu-P Coatings. *Journals of Electrochemical Society*. 150(11): C760-C764.

[4] Narayanan, T. S. N. Sankara, Selvakumar, S. and Stephen, A. 2003. Electroless Ni-Co-P Ternary Alloy Deposits: Preparation and Characteristics. *Surface & Coatings*. 172: 298-307.

[5] Osaka, T. 1992. Electrochemical Aspects of Advanced Electronic Materials. *Electrochimica Acta*. 37(6): 989-995.

[6] Zaimi, M. and Noda, K. 2013. Effect of Coating Thickness on Corrosion Behavior of Electroless Quaternary Nickel Alloy Deposit in 3.5wt% NaCl Solutions. *Journal of Advanced Manufacturing Technology*. 8(2): 83-92.

[7] Abrantes, L. M. and Correla, J. P. 1994. On the Mechanism of Electroless Ni-P Plating. *Journals of Electrochemical Society*. 141(9): 2356-2360

[8] Cui, G., Liu, H., Wu, G., Zhao, J., Song, S., amd Shen, K. S. 2008. Electrochemical Impedance Spectroscopy and First-Principle Investigations on the Oxidation Mechanism of Hypophosphite Anion in the Electroless Deposition System of Nickel. *Journals of Physical Chemistry C*. 112: 4601-4607.

[9] Hung, A. and Chen, K. 1989. Mechanism of Hypophosphite-Reduced Electroless Copper Plating. *Journals of Electrochemical Society*. 136(1): 72-75.

[10] Toda, A., Chivavibul, P. and Enoki, M. 2013. Effects of Plating Conditions on Electroless Ni-Co-P Coating Prepared from Lactate-Citrate-Ammonia Solution. *Materials Transactions.* 54(3): 337-343.

[11] Zaimi, M., Azran. M. N., Khaizaki, M., Alif, M., Aziz, M. S. A., Azam, M. A., Kasim, M. S., Munawar, R. F. and Abd Manaf, M. E. 2016. Electroless Ni-Co-Cu-P Alloy Deposition in Alkaline Hypophosphite Based Bath. *Key Engineering Materials*. 694: 151-154.

[12] Chassaing, E., Cherkaoui, M. and Srhiri, A. 1993. *Journals Applied Electrochemistry*. 23: 1169-1174.

[13] Abdel Aal, A., Shaaban, A. and Hamid, Abdel 2008. Nanocrystalline Soft Ferromagnetic Ni-Co-P Thin Film on Al Alloy by Low Temperature Electroless Deposition. *Applied Surface Science*. 254: 1966-1971.

[14] Van den Meerakker, J. E. A. M. 1981. On the Mechanism of Electroless Plating. II. One Mechanism for Different Reductants. *Journals Applied Electrochemistry*. 11: 395-400.

[15] Bounanani, M., Cherkaoui, M., Cherkaoui, M., Belcadi, S., Fratesi, R. and Roventi, G. 1999. Ni-Zn-P Alloy Deposition from Sulfate Bath: Inhibitory Effect of Zinc. *Journals Applied Electrochemistry*. 29: 1171-1176.

[16] Lee, Chwan-Ying and Lin, Kwan-Lung 1994. Ni-Cu-P and Ni-Co-P as a Diffusion Barrier between an Al Pad and a Solder Bump. *Thin Solid Films*. 239: 93-98.

[17] Balaraju, J.N., Radhakrishnan, Praful, Ezhilselvi, V., Kumar, A. Anil, Chen, Zhong and Surendran, K.P. 2016. Studies on Electroless Nickel Polyalloy Coatings over Carbon

Fibers/CFRP Composites. *Surface & Coatings Technology*. 3302: 389-397

[18] Sudagar, Jothi, Lian, Jianshe and Sha, Wei 2013. Electroless Nickel, Alloy, Composite and Nano Coatings – A Critical Review. *Journals of Alloys and Compounds.* 571: 183-204.

[19] Sahoo, Prasanta and Das, Suman Kalyan 2011. Tribology of Electroless Nickel Coatings – A Review. *Materials & Design*. 32(4): 1760-1775.